



**HAL**  
open science

## Design of a low frequency, impulsive sound simulator in an existing house for sonic boom perceptual studies

Léo Cretagne, Carlos Garcia A., Roman Leconte, François Ollivier, Jacques Marchal, Frédéric Marmel, Claudia Fritz, François Coulouvrat

### ► To cite this version:

Léo Cretagne, Carlos Garcia A., Roman Leconte, François Ollivier, Jacques Marchal, et al.. Design of a low frequency, impulsive sound simulator in an existing house for sonic boom perceptual studies. *Acta Acustica*, 2023, 7, pp.61. 10.1051/aacus/2023057 . hal-04339448

**HAL Id: hal-04339448**

**<https://hal.science/hal-04339448v1>**





Submitted on 13 Dec 2023

**HAL** is a multi-disciplinary open access archive for the deposit and dissemination of scientific research documents, whether they are published or not. The documents may come from teaching and research institutions in France or abroad, or from public or private research centers.

L'archive ouverte pluridisciplinaire **HAL**, est destinée au dépôt et à la diffusion de documents scientifiques de niveau recherche, publiés ou non, émanant des établissements d'enseignement et de recherche français ou étrangers, des laboratoires publics ou privés.



# Design of a low frequency, impulsive sound simulator in an existing house for sonic boom perceptual studies

Léo Cretagne, Carlos Garcia A. , Roman Leconte, François Ollivier, Jacques Marchal, Frédéric Marmel<sup>a</sup> , Claudia Fritz\* , and François Coulouvrat 

Institut Jean Le Rond d'Alembert, Sorbonne Université, CNRS UMR 7190, 4 place Jussieu, 75005 Paris, France

Received 26 April 2023, Accepted 19 October 2023

**Abstract** – The renewal of civil supersonic aviation is partly conditioned by the establishment of an international regulation on sonic boom level. Human perception of booms from future aircraft creating sound disturbances of lower level than past ones can currently be evaluated only through boom simulators in laboratory setups with predicted signatures from numerical simulations. To reach sufficient ecological validity, it is necessary that perception studies take place in an environment as familiar as possible to participants. With this in view, a simulator has been designed to reproduce sonic booms of low amplitude with the highest possible fidelity and control, while adapting to an existing house. The article presents the challenges and design solutions chosen to reach this objective. A double optimisation of the input signal, successively in the frequency and in the time domain, is described. Observed performances are presented for different boom exposures and in various rooms of the house.

**Keywords:** Sonic boom, Simulator

## 1 Introduction

Sonic boom is one of the main barriers to the renewal of civil supersonic aviation, twenty years after Concorde's last flight. The loud and sudden double booms (associated to shocks emanating one from the aircraft nose and one from its aft) it produced all along its supersonic cruise made overland flights unacceptable and restricted Concorde service to transatlantic routes. This also led many countries in the 70's to strictly forbid any civil supersonic overland flight. Following pioneering theoretical works [1–3] based on fundamental Whitham's theory of sonic boom [4], tremendous progress has however been achieved in the design of supersonic aircraft to significantly reduce sonic boom noise level at the ground. The Shaped Sonic Boom Demonstration (SSBD) American program demonstrated in 2003 for the first time in-flight boom mitigation by modifying the aft-fuselage of an F-18 fighter [5]. The Japanese D-SEND program [6] measured and compared the boom levels of two dropped bodies of revolution, one of which with a low boom design. At NASA, the X-59 Quiet Supersonic Technology demonstrator) is currently in testing phase to reach a ground boom Perceived Level [7] of 75 PLdB in standard

atmosphere [8]. It should validate technologies for reducing sonic boom loudness.

Human response to N-like booms or to shaped booms of lower levels can be evaluated through data gathered by means of either laboratory, in-home or field studies. Field studies take place in a normal listening environment, but lack details about the precise sound exposure. In contrast, laboratory studies provide the highest control of sound exposure but take place in a very abnormal listening environment [9]. Maglieri et al. [10] reviewed seven of these environments designed since 1965 to reproduce sonic booms of high amplitude with a high control. Most of them are tiny airtight pressure chambers surrounded by multiple loudspeakers, such as the NASA booth [11] with a volume of 1.6 m<sup>3</sup> for only one seated person. Such technology was used recently in Japan [12], and in Germany [13]. A larger portable chamber was developed by Gulfstream for demonstration purposes [14]. It was installed in a mobile trailer, offering a larger volume for four standing people. The trailer was used as a waveguide with an anechoic termination efficient above 50 Hz. Consequently, only a band-pass filtered waveform could be reproduced. However, the realism of the boom reproduction was judged somewhat superior for this system compared to smaller chambers [15]. Paradoxically, all these narrow chambers are best suited for investigating outdoor boom responses. An indoor boom will be affected by specific construction features of walls, roofs, doors and primarily windows, and also by interior layout.

<sup>a</sup>Frédéric Marmel is now at WS Audiology, ORCA Europe, Stockholm, Sweden.

\*Corresponding author: [claudia.fritz@sorbonne-universite.fr](mailto:claudia.fritz@sorbonne-universite.fr)

House shaking, rattle noise and damage concerns were actually identified as the main factors influencing human response to sonic booms (see for reviews: [10, 16, 17]). Human response may also be dependent on what the person is doing at the time of boom exposure. All these effects cannot be investigated inside tiny pressure chambers.

Therefore, in-home studies with sonic booms reproduced through arrays of loudspeakers appear as an appealing compromise between the highly artificial listening environment of pressure chambers and costly community surveys with poor quantitative information on noise exposure. In-home studies allow a good control of sound exposure and a realistic environment, closing in on the so-called “ecological validity” [18, 19]. They are currently all the more appealing as low-boom aircrafts do not exist yet, and low amplitude sonic booms result only from numerical simulations of putative supersonic aircrafts. In addition, in-home studies are more likely to reproduce some other factors that have been shown to be key ingredients of human indoor response. In a 1993 study (published in [20]), an array of 3 or 4 loudspeakers played a randomly pre-programmed sequence of three different boom waveforms in the range 66–74 dBA (ASEL) with a total of 4–63 booms per day. The system was installed inside the homes of 33 participants along with 2 microphones measuring the sound signal. The low number of loudspeakers and their limited bandwidth led to a sound reproduction far from a sonic boom shape. More recently [21], NASA built in its Langley Research Center a large size simulator designed for studying indoor boom. A single blind room ( $4.09 \times 3.45 \times 2.54 = 35.84 \text{ m}^3$ ) facility, built using typical US residential construction methods and materials, is surrounded by two arrays of loudspeakers close to two of the exterior walls, with a total of 52 subwoofers and 52 mid-range speakers, so that outdoor booms can be transmitted indoor through one or two room walls, one with a closed window. However, even if the interior has been designed with care to resemble a living room, this facility remains somehow artificial (a single blind room) and is not representative of European homes. Note also that insonifying directly an entire existing house by an array of loudspeakers has been examined but turned out to be very challenging and was never realised [22].

This motivated the present study, which aimed at developing a system (consisting in two simulators) that is able to reproduce sonic booms in different rooms of an existing house, and not in the artificial laboratory environment, in order to investigate the influence of low sonic booms on humans in natural conditions.

## 2 Description of the house

The test house is located (GPS position  $+48.800170^\circ$ ,  $-2.075682^\circ$ ) at the entrance of one campus of Sorbonne Université located about 21.5 km southwest from Paris Notre Dame. The test house (Fig. 1, top) is a three storey building plus a basement, uninhabited during the study. The house was constructed in the late 19th century with thick concrete walls and large single pane windows. The

ground floor used for the study (Fig. 1, bottom) is occupied by a single apartment made of three bedrooms, one living room, one kitchen and one bathroom with toilets. The volumes are:  $29.8 \text{ m}^3$  for bedroom 1 situated on the house front,  $34.0 \text{ m}^3$  for bedroom 3,  $72.9 \text{ m}^3$  for the living room and  $40.2 \text{ m}^3$  for the kitchen. The dimensions and the reverberation times of the four rooms are provided in Appendix A. A side door in the kitchen, opening directly into the garden, produces strong rattle when loosely fitted.

## 3 Properties of chosen low boom signals

### 3.1 Signals to be reproduced in the bedrooms for a sleep study

The two boom simulators were first designed for a night noise study, with participants sleeping in the (closed) bedrooms 1 and 3. To this end, five different target outdoor low boom signals have been selected (Fig. 2) to be reproduced with fidelity as high as possible. Their peak overpressure is around 20 Pa, one fifth of Concorde’s pressure. There is no consensus yet on the best metric(s) to quantify human response to low boom exposure, but, following a meta-analysis of annoyance studies performed in the USA and Japan [23] 6 metrics have been pre-selected by Super-Sonic Transport Group (SSTG) of Committee on Aviation Environment Protection (CAEP) from International Civil Aviation Organisation (ICAO): Sound Exposure Level (SEL) with 4 different (A, B, D, E) frequency weightings (though C-weighting was not retained due to its poor correlation with outdoor ratings, it is here indicated as frequently recommended for indoor low frequency noise), Stevens Mark VII Perceived Level (PL) [7] and ISBAP, a hybrid metric combining PL, CSEL and ASEL. Peak overpressure and boom levels for the 6 metrics pre-selected by ICAO plus CSEL are provided in Table B1 in Appendix B.

The five selected signals (booms 1–5, ordered by increasing level in terms of metrics ASEL, BSEL, DSEL, ESEL and PL) show a level range of about 23 dB, both in terms of dBA (ASEL) and PL. Signal 2 corresponds to the ground signal of C25P low boom notional configuration cross-investigated during the 2nd AIAA Sonic Boom Workshop [24] with a sound level of 76.2 PL dB (61.7 dBA) close to the announced 75 PL dB of the X59 NASA demonstrator. Signal 5 shows the typical N-waveform. Compared to boom 2, a sharper shock leads to a wider-band signal with frequency content sharply decreasing only beyond 1000 Hz and its sound level is 17 dB higher for ASEL metric, and 15.5 dB higher for PL metric. Booms 1 and 4 are derived respectively from signals 2 and 5 after having undergone a numerically simulated propagation through one kilometre of synthetic atmospheric turbulence [25, 26]. This leads to energy losses for frequencies above 300 Hz from signal 2 to signal 1, thus reducing the boom sound level by about 7 dB for both PL and ASEL. Compared to signal 5, signal 4 propagated through a random caustic (a zone of local sound amplification produced by the random distortion of the wavefront due to turbulence), displaying the typical superposition of a U wave to the initial N wave. This reduces its

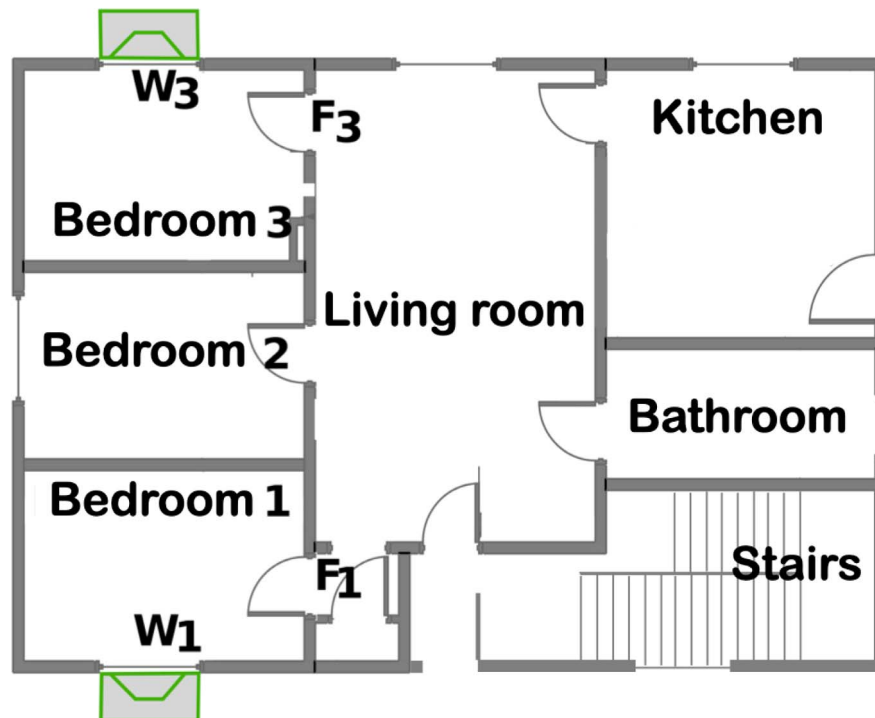


**Figure 1.** Top: front view of the test house, with one boom simulator affixed to the ground floor window of bedroom. Bottom: map of the ground floor apartment with the position of the two simulators (in green) affixed to windows W1 and W3.

frequency content above 400 Hz, and its level falls off by 4.5 (ASEL) to 5 (PL) dB. Signal 3 was measured from an F18 airplane executing a low boom dive manoeuvre. Its peak overpressure, duration and frequency peak are similar to those of signals 4 and 5, but its shape is different with smoother shocks and a bumpy waveform. In the mid frequency range 30–500 Hz, its spectrum decays faster. This explains its lower ASEL level (−5 and −9.5 dBA, respectively), though the difference in PLdB is much less (−1.4 PLdB compared to boom 4).

In Figure 2 we also report the spectrum of background noise measured over a 2 s duration just before boom generation and recording. When discarding the few peaks related to electrically induced hum noise, all spectra decay

towards higher frequencies, reaching a plateau above 100 Hz at around 15 dB. For all target signals, this noise level is well below the signal level in the low frequency part below 100 Hz (−50 dB or more at the peak of the spectrum). Above 100 Hz, the difference reduces all the faster as the signal is of lower noise level, e.g., has a lower high frequency content that merges with the background noise (around 450 Hz for boom 1 but around 2000 Hz for boom 5).

### 3.2 Signals to be reproduced in the living room for a day study

In addition to the sleep study, the simulators were intended to be used as well in a day study with participants



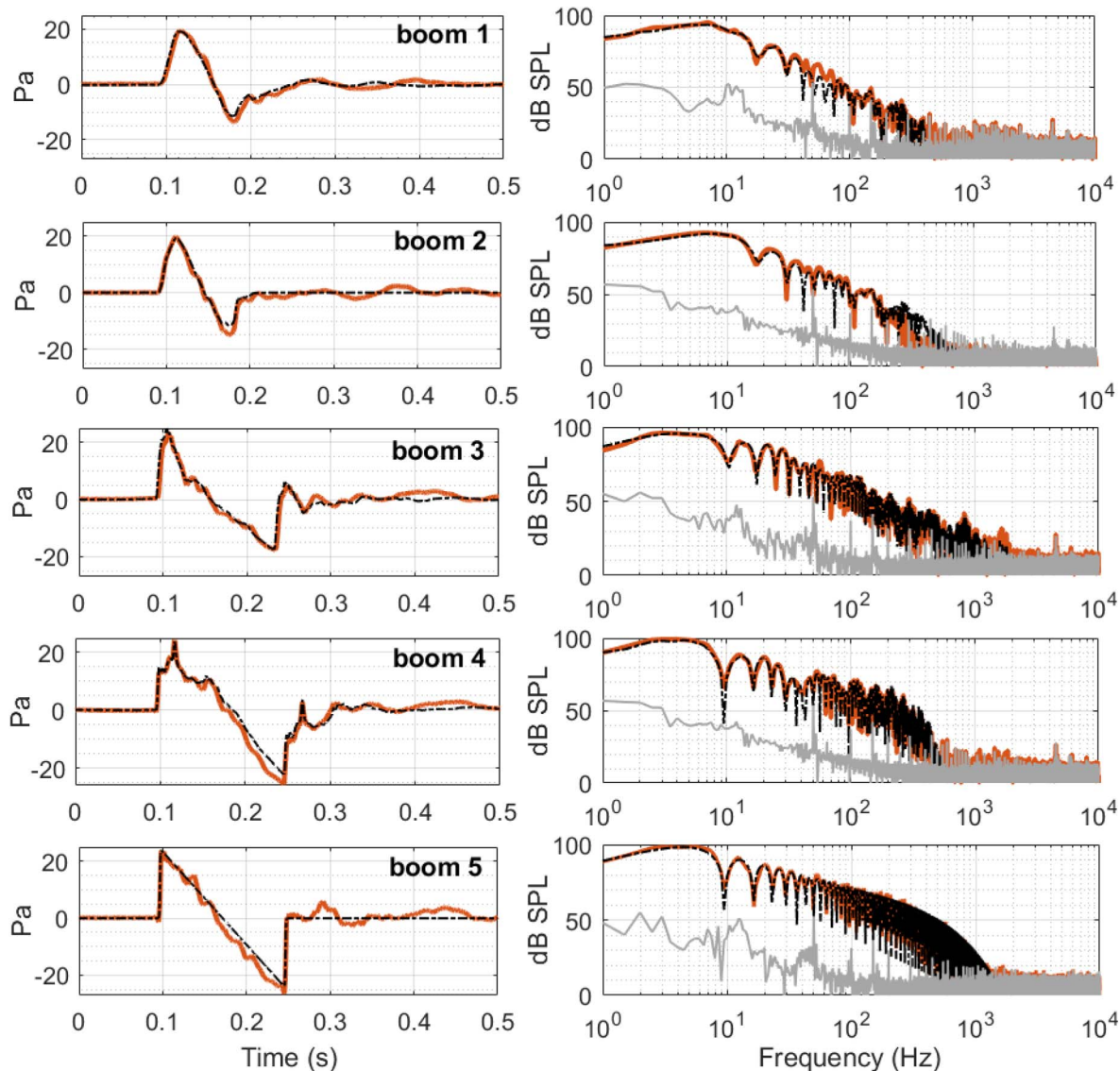


**Figure 2.** Temporal waveforms (left) and frequency spectra (right) of selected boom signals ordered by increasing A-SEL values from top to bottom (booms 1–5). Comparison between the target signals in dotted black and the measured signals at the centre of the window frame W3 in closed bedroom 3 in solid red. Lower curves in light grey show ambient noise spectra measured during 2 s.

involved in various activities. For such study, a bedroom with a wide open window fully obscured by the simulator could have appeared as an unusual or even disturbing environment. Our goal was thus to synthesise booms inside the living room with natural daylight and with the simulators not directly visible. However, each simulator was dimensioned to insonify one bedroom, of much smaller volume. Operating the two simulators simultaneously would not have been sufficient to compensate for the increased volume of the two bedrooms plus the living room ( $103.7 \text{ m}^3$ ). The 12 subwoofers used for the two bedroom simulators could have been spread in front of the two inner (open) doors between the living room and the bedrooms, but this would have i) made the simulators visible again, ii) only partially compensated for the increased volume, and iii) required a new design of the whole system installation. For the sake of simplicity and time and money saving, we made the

choice to keep the simulators unchanged and used the two (now open) doors (F1 and F3, Fig. 1) between the living room and the bedrooms as “virtual windows”, through which the booms would insonify the living room. Note that door and window areas are very similar. Target boom signals needed however to be modified in order to be able to insonify a much larger volume considering the maximum power available from our system. Their peak amplitude is slightly reduced (to about 17–18 Pa) and only N-wave profiles are considered (see Fig. 3) with rise times adjusted to reach two desired boom level: 62 dBA (or 78 PLdB) and 75 dBA (or 88.4 PLdB). The first additional signal (boom 6), subsequently also called Low Boom signal, is purposely chosen so that its various metrics are comparable to those of signal 2 (C25P), while the second one (boom 7), called High Boom, is significantly louder (+13 dBA or +10 PLdB) with the same duration. Their spectra,

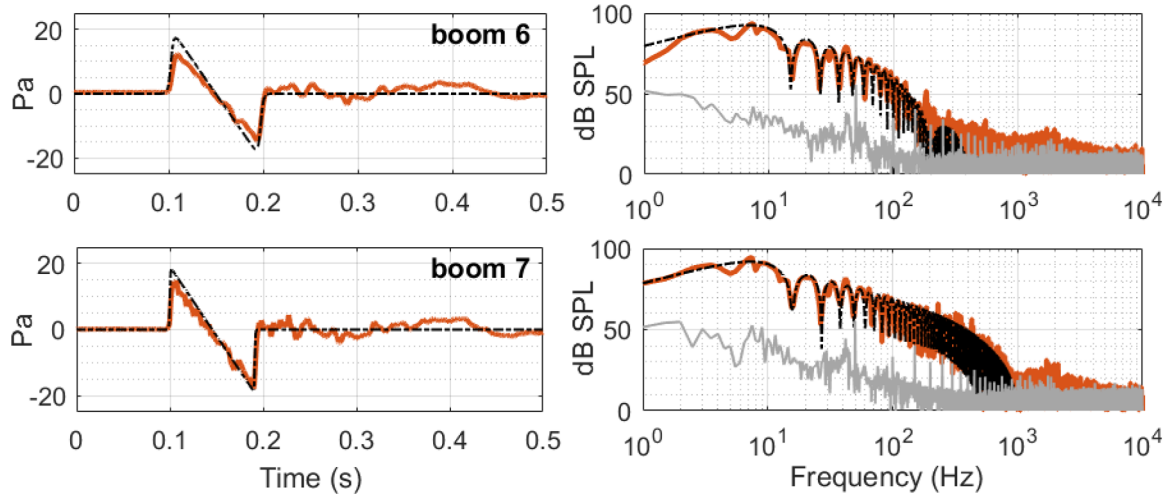


**Figure 3.** Comparison between the target signals (N-wave like booms, in dotted black) and the measured signals (in solid red) at the door F3 between bedroom 3 and the living room, generated by simulator 3. Top: low boom signal 6. Bottom: high boom signal 7. Left: temporal waveforms. Right: frequency spectra. Measured spectra are noisier and decay much slower in the high frequency limit. Lower curves in light grey show ambient noise spectra measured during 2 s.

displayed on Figure 3, show similarities at low frequencies, with higher frequency content above 50 Hz decaying more rapidly for the lower boom signal.

#### 4 Design of the boom simulators

To reach highest possible fidelity, the sound reproducing system, or simulator, had to be capable of producing very low frequencies signal (down to at least 1 Hz or even below) at a pressure level up to 25 Pa (or 122 dB overall sound pressure level) while also covering the audio range up to around 1 kHz (above, the ambient noise is dominating, see Fig. 2). Temporal accuracy was also critical for strongly impulsive signals. Also, neighbour disturbances were to be strictly avoided. Considering the house described above, we chose to insonify from outdoor only two of the ground floor bedrooms by means of a sound system affixed to each window frame (see Fig. 1). By taking advantage of the bedrooms limited volume, the required number of loudspeakers was significantly reduced to seven per bedroom. For the simulator design, it was assumed that each bedroom behaved as a completely airtight pressure chamber. The window opening was made fully airtight by affixing the simulator to outer walls with foam (see details below). The door however had to be left unmodified and was the main source of sound leakage. It could however be compensated, as it will be proved later on by comparison between target and measured signals. The most energetic part of the boom frequency spectrum is at wavelengths which are very large (typically 45 m for the peak frequency) compared to the room dimensions (3.85 m for the largest one). Thus the pressure inside the room is homogeneous and can be approximated for a loudspeaker-like sound source in the frequency domain by  $p(\omega) = \rho_0 c_0^2 x(\omega) S_d / V$  where  $\rho_0$  is the air density,  $c_0$  the sound velocity,  $\omega$  the angular frequency,  $V$  the room volume,  $S_d$  the surface of the sound source and  $x(\omega)$  the membrane excursion. For the considered bedroom

volume of 30 m<sup>3</sup>, a pressure amplitude of 25 Pa was obtained inside the room with a sound source reaching the volume change  $x(\omega) S_d = p(\omega) V / \rho_0 c_0^2 = 0.0054$  m<sup>3</sup>. The maximal membrane excursion should also remain in the linear range to avoid any distortion. We thus chose the B&C Speaker 21SW115 loudspeaker with a membrane surface of 1680 cm<sup>2</sup> and a linear excursion limit of 10 mm. Six of them were needed to reach the target boom level. To reproduce the signal high frequency content for which no simple relation between pressure signal, loudspeaker parameters and room volume exists, we added a more conventional wide-band loudspeaker (Beyma 8BR40N) in the audible range (60–6000 Hz), enough to radiate the medium and high frequency part of the spectrum up to typically 1500 Hz (for instance sound level at 100 Hz is about –50 dB compared to the peak value around 5–7 Hz). Above this frequency, the signal amplitude reached the level of the ambient noise existing in the house (ranging between 10 and 20 dB SPL) and no precise control was therefore possible. Moreover, it has been shown that the various boom metrics get almost insensitive to the part of the spectrum above 1500 Hz ([26], Fig. 15).

The cabinet was designed to optimise the very low-frequency response of the system while presenting the most accurate temporal response. To avoid any rear-side sound radiation we use a closed-box design, which presents a second order roll-off slope and almost the same qualities as an infinite baffle design, except for the acoustic stiffness added by the enclosure volume which modifies the resonance frequency of the loudspeaker. Two identical cabinets were installed outdoor, one right at the window frame of each bedroom (see Fig. 1). The cabinets were made of 18 mm fireproof plywood, assembled by a grooved and glued joinery technique, and protected with waterproof white paint reflecting sunlight to prevent the wood to stretch or deform under heat. The complete structures were attached to the house outer walls with polyurethane expensive foam,



**Figure 4.** Cabinet design. Left drawings: installation of the loudspeaker, six subwoofers and their back volumes (top, front, side and 3D views). Right photograph: simulator viewed from inside the bedroom.

providing air tightness. Each cabinet was separated into six identical compartments of 200 L each, leading to a critically damped alignment of the subwoofers. The wide-band loudspeaker had its own, smaller, back volume (150 L) of different shape, again for critically damped alignment. The loudspeaker back volume was filled with acoustic foam, so as to dampen internal resonance modes and reflections. The dimensions of the cabinets and the operating frequency band (1–100 Hz) of the subwoofers were too small to create internal modes or noticeable reflections inside the subwoofers back volumes. In case the subwoofers would produce harmonic distortion, the same acoustic foam was also used in each back volume. The speakers were facing into the bedrooms (see Fig. 3), with the cabinet dimensions exceeding those of the window frame (2.16 m × 1.3 m) to allow easy outdoor sound insulation. The window frames were smaller than the overall surface of all speakers, so that the subwoofers were orientated out of the window planes. This actually provided a better balance of the cabinet structure (supported by an aluminium frame with adjustable feet height) and prevented them from shaking due to subwoofers stroke. The total weight of the 6 subwoofers alone was 84 kg, the overall weight of one simulator around 200 kg. Electrical wiring was designed so that only one big cable (8 tracks cable) was plugged to each cabinet via one SpeakOn weatherproof connector placed on the outdoor side of the cabinet, with no cable inside the bedrooms. The overall design and cabinet installation are illustrated in Figure 4.

To get the required 300 W of electrical input – estimated in a conservative way by using the measured free field sensitivity of the subwoofers (97 dB.W<sup>-1</sup>.m<sup>-1</sup>) and the distance between the microphone and the centre of the two upper, most distant subwoofers (approximately 1 m, see Fig. 4), we used power amplifiers BEAK BAA

800, delivering 800 W of audio signal down to DC at a 4 Ω load with a very low output distortion (<0.1%). Two subwoofers, wired in parallel, were paired and fed by one amplifier, thus requiring a total of six amplifiers for the two simulators. The wide-band loudspeakers were powered by one BEAK BAA 120 amplifier, presenting the same characteristics as the BEAK BAA 120 except a reduced nominal power (120 W). A NI USB 9260 signal generator, featuring two BNC outputs and operating audio signals from DC up to 23 kHz with a resolution of 24 bits, was used: one output passively split the signal going to all the 12 subwoofers through the 6 amplifiers, while the other one drove the two wide-band loudspeakers through their own amplifier. The electroacoustic chain is illustrated in Figure 5.

## 5 Signal generation

### 5.1 Optimisation principle and measurement equipment

For the sleep study, the simulated signals produced by the boom simulator were optimised at the centre of bedroom 3’s window frame (W3 in Fig. 1), with the door closed, so as to insonify a small volume. For the day study, the input signals were optimised for each simulator at the middle of the corresponding bedroom door (F1 or F3, see Fig. 1), all other doors being closed.

Optimisation was achieved by recording the signal at a single point, either the centre of the window frame or the bedroom door, with a Bruël & Kjaer type 4964 microphone (equipped with a low frequency pre-amplifier adapter type UC-0211) operating with a flat frequency response from 0.02 Hz up to 20 kHz, connected to a Bruël & Kjaer NEXUS type 2690 microphone conditioner and a NI USB 4431 acquisition card operating from DC up to 43.5 kHz



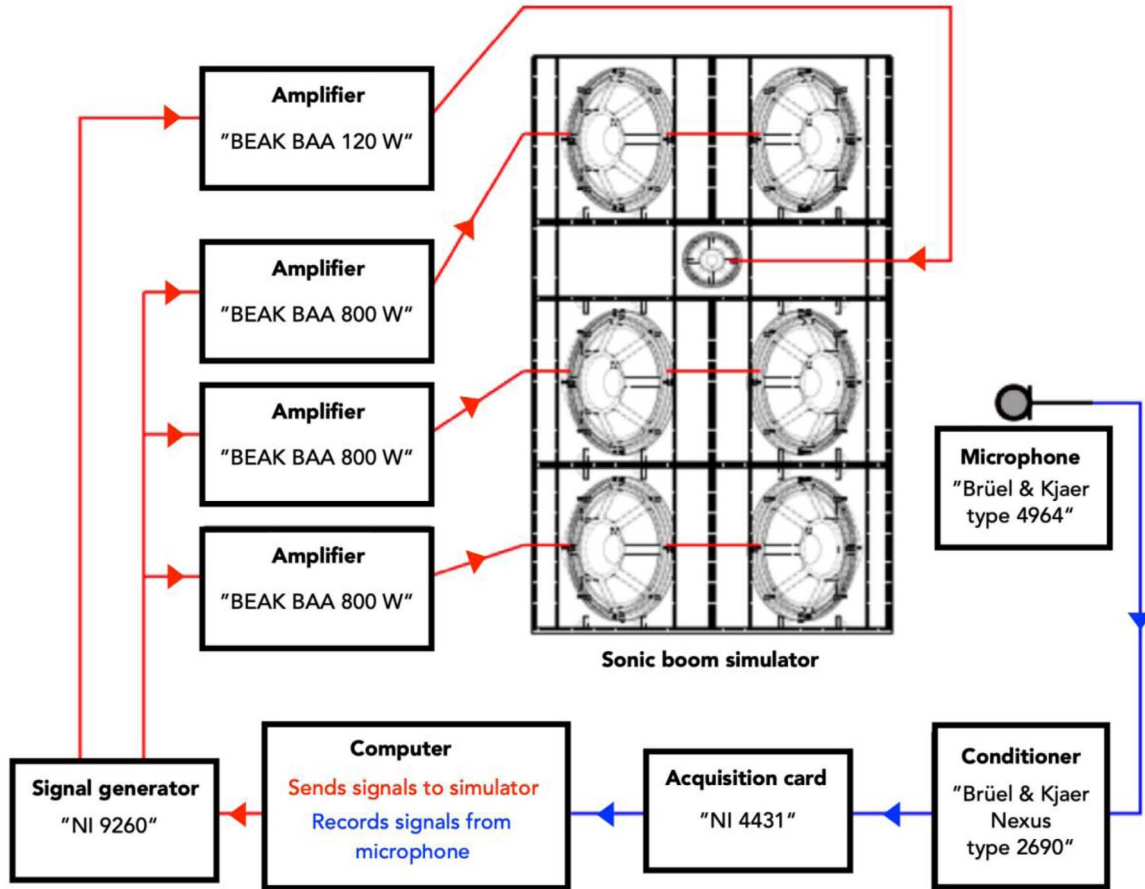


**Figure 5.** Diagram of the electroacoustic chain: in red, the chain corresponding to the generation of the signals; in blue the measurement chain used for the optimisation of the signals (see Sect. 5).

on 24 bits. A single computer operated the signal production and recording via a Matlab program, as illustrated in Figure 5.

## 5.2 Optimisation method

For the optimisation process, the signal is separated into a low frequency component generated by the subwoofers, and a medium/high frequency one generated by the other loudspeaker. The frequency response of the subwoofers and the wide-band loudspeakers are flattened using a standard equalisation process. In addition, the low frequency component is optimised in the time domain, using the so-called Wave Decomposition Technique (WDT). This non-iterative method was initially proposed by Tokuyama et al. [27] to optimise, at one microphone position, an impulsive signal (namely a sonic boom) reproduced by an electroacoustic system. WDT was then extended by Blanc et al. [28] to the case of several microphones. We here apply the method in the original case of a single microphone. The only difference is that WDT method is only applied to the low frequency part of the signal reproduced by the subwoofers, which is quite homogeneous inside the room. Applying the WDT to the high frequency part in a reverberating room with multiple arrivals at high frequencies would induce artefacts.

All time signals are denoted by lower case letters, with  $c(t)$  the target (“cible” in French) time signal,  $s(t)$  the input signal at the simulator, and  $m(t)$  the measured signal at the single selected microphone position. For any time signal  $f(t)$ , we note its time discretisation  $f_i = f(i\Delta t)$  with  $i = 0$  to  $n$ , and its Fourier transform by  $F(\omega) = \mathcal{F}(f(t))$  with  $\omega$  the angular frequency. Low and high frequency parts are denoted by indexes, respectively  $<$  and  $>$ . To separate these two parts, we use a low pass, second-order Butterworth filter noted  $B_{<}(\omega)$  centred at 100 Hz ( $-3$  dB cut-off frequency). A mirror high pass, second order, Butterworth filter  $B_{>}(\omega)$  again centred around 100 Hz is used to filter the low frequencies sent to the loudspeakers. The intermediate frequency range (50–200 Hz) corresponds to the common bandwidth between the loudspeaker and the subwoofers. Therefore  $c_i(t) = \mathcal{F}^{-1}(B_i(\omega)C_i(\omega))$  for  $(i = <, >)$ . Such smooth, second order filters avoids a sharp LF/HF split that would distort the time signal.

For frequency equalisation, the impulse responses of the low frequency (subwoofers) and high frequency (loudspeaker) chains were measured. A known wide band signal (Heaviside function)  $h(t)$  is split similarly into its two low and high frequency components  $h(t) = h_{<}(t) + h_{>}(t)$ , each one being sent to the corresponding outputs of the generation card. The resulting measured signals (via the microphone at the centre of the window frame)  $w_{<}(t)$  and



$w_{>}(t)$  provide the LF and HF impulse responses of the system  $R_i(\omega) = W_i(\omega)/H_i(\omega)$  for  $(i = <, >)$ . Equalisation is achieved by generating the input signals  $s_i^E(t) = \mathcal{F}^{-1}(C_i(\omega)/R_i(\omega))$  for  $(i = <, >)$ , thus creating a Finite Impulse Response (FIR) filter. The corresponding signals measured at the selected microphone position are respectively  $m_{<}^E(t)$  and  $m_{>}^E(t)$ .

The WDT method is then applied, modifying the input signal  $s_{<}^E(t)$  to minimise the deviation between  $m_{<}^E(t)$  and  $c_{<}^E(t)$ . A basis of time waveforms is created by shifting the measured signal by a constant time delay  $jM\Delta t$ , so that  $b_j(t) = m_{<}^E(t - jM\Delta t)$  with  $j = 0$  to  $N$ . This leads to  $b_{jk} = (m_{<}^E)_{i-Mj}$ . Here  $M$  is chosen equal to 3, and  $N$  so that the beginning (first shock for an N-wave) of the most shifted signal  $b_N$  is slightly beyond the end (second shock of an N-wave) of the target. When  $-Mj < 0$ , the value 0 is assigned (impulsive signal vanishing before its initial shock). The target signal  $c_{<}(t)$  is decomposed onto this basis,

$(c_{<})_i = \sum_{k=0}^N a_k b_{jk}$ , the coefficients  $a_k$  being found by least square minimisation. A second basis is created by shifting the target signal  $c_{<}(t)$  by the same constant time delays so that  $d_{jk} = (c_{<})_{i-Mj}$ . The time discretised, low frequency, input signal after WDT optimisation is  $(s_{<}^W)_j = \sum_{k=0}^N a_k d_{jk}$ .

This signal is again frequency-equalised as previously described, and the resulting low frequency signal sent to the amplifiers is  $s_{<}^{WE}(t) = \mathcal{F}^{-1}(S_{<}^W(\omega)/R_{<}(\omega))$ .

### 5.3 Reproduction results

#### 5.3.1 In bedrooms 1 and 3

The results of the optimisation at the centre of the window frame for bedroom 3 insonification are illustrated on [Figure 2](#), by comparing the five target signals described earlier (in black) to the measured ones (in red). Note that waveforms are shown over a 0.5 s duration, but spectra and metrics were computed on a 2 s interval. After WDT application, the measured time waveforms almost perfectly match the target ones. The comparison of frequency spectra also outlines excellent agreement, some tiny mismatches appearing mostly in the range 50–100 Hz where the subwoofers and the loudspeaker are operated simultaneously and also where background noise shows some peaks. Measured post-boom signals also display some decaying oscillations of low amplitude and low frequency, as a result of the inertia of the subwoofers which cannot be immediately stopped after the rear shock. Distortions measured here are anyway much smaller than those frequently produced by atmospheric turbulence [[26](#), [29](#)], and the realism of the synthesised booms is therefore highly satisfying. Also noticeable is the good agreement in phase, particularly visible on the time waveform of boom 4, which is a superposition of an N-wave with two shocks and of a U-wave (which is an N-wave having undergone a  $\pi/2$  phase shift) with two peaks, all arriving at the same time as the target. When comparing the metrics of the measured booms to the target ones (see [Table B1](#) in [Appendix B](#)), an overall good

agreement is obtained, with mean deviations of about +0.8 dB. It ranges between +0.1 dB and +0.5 dB for all SEL metrics while mean PL difference reaches 2.3 dB. This poorer agreement for the PL metric is mainly due to boom 1 (for which the agreement is poorer for all metrics anyway with a mean deviation of 2.8 dB). This could indicate that the PL metric magnifies the influence of the background noise, as boom 1 is of smaller amplitude, and thus the signal-to-noise ratio is lower (its spectrum level is comparable to ambient noise at frequencies as low as 500 Hz).

#### 5.3.2 In the living room

The synthesised booms 6 and 7 measured at the virtual window F3, with only simulator 3 working, are compared to the targets on [Figure 3](#). The overall N-like boom shape is well reproduced, and the rise time differences between the Low and High Boom signals are clearly visible. However, as the system is reaching its limit to insonify a big volume, the measured peak overpressure is slightly lower than the target, the low frequency spectrum shows some mild oscillations and the high frequency spectrum decays more slowly than the target to compensate, in terms of dB, the reduced peak pressure. Also post-boom noise is somewhat more important than for booms synthesised in the bedrooms. Nevertheless, the measured signals clearly had the characteristics of a sonic boom signal: impulsive signals with two sharp shocks separated by an expansion wave, and a wide-band spectrum peaking around 7 Hz. Deviations from the target are comparable to what can be measured outdoor in case of a mild turbulence [[29](#)]. Regarding metrics, agreement is typically within 1 dB mismatch, except again for the PL value of the Low Boom case.

### 5.4 Discussion and limitation

This section compares our boom simulator to the two most recently designed ones, with the data being summarised in [Table 1](#). The two simulators are actual pressure chambers, a small one at University of Oldenburg (Germany) for assessing outdoor boom [[30](#)] and the NASA indoor boom simulator [[21](#)], an American-style living room enclosed in a large pressure chamber with numerous loudspeakers (104). For this last one, indoor boom is transmitted through the room closed window and two of its walls. Let us recall that our simulator aims at reproducing indoor booms assumed to be transmitted through one (for the bedroom) or two (for the living room) wide-open windows, neglecting transmission through walls assumed to be stiff enough. The number of loudspeakers is therefore reduced to either 7 or 14, in order to control the signal on the window surface only. We here explored only a limited number of waveforms (5 for the bedroom, 2 for the living room) with one amplitude for each and with levels varying in the range 56–92 dBA (ASEL) or 76–92 PLdB. This range is larger than the one explored in Germany and smaller than the one of US simulator. Higher amplitudes are of limited interest because of the progresses made in low boom design. Smaller amplitudes could have been explored here (by just reducing the overall signal amplitude), but in this case one

**Table 1.** Summary of data comparing 3 types of simulators – 1st column: acronym of the institution (NASA: National Aeronautical and Space Administration, USA, [21]; OLD: University of Oldenburg, Germany, [30]; SU: Sorbonne Université, present article) – 2nd column: type of reproduced booms – 3rd column: volume of the room in cubic meters – 4th column: number of loudspeakers – 5th column: number of different reproduced booms – 6th column: accuracy of the reproduction (min and max differences in dB between reproduced and target boom, first line in ASEL, second line in PL) – 7th column: range of reproduced outdoor booms (first line in ASEL, second line in PL). Indoor boom levels are different. NP: data not provided in the reference.

Simulator	Type of boom	Vol.	# LS	# Booms	Accuracy	Range
NASA	Indoor (transmission through walls and closed window)	36	104	73	NP −0.7 to +0.6	NP 70–105
OLD	Outdoor	9	2	24	NP NP	55–70 NP
SU (bedroom)	Indoor (transmission through open window)	34	7	5	−0.1 to +0.9 +0.5 to +6.8	56–78 76–92
SU (living room)	Indoor (transmission through 2 open windows)	73	14	2	−0.1 to +1 +0.8 to +2.7	62–75 81–89

faces the issue of background noise level which, though small, is significantly higher in a real existing house than in a laboratory pressure chamber. This raises several open questions: i) which metric is most/less sensitive to noise? ii) how much does background noise influence boom perception? iii) how to control accurately a simulated boom independently of the background noise? Our present results indicate preliminary trends. First, PL metric (and therefore ISBAP) seems to be more sensitive to background noise than SEL metrics, due to its nonlinear character (dependent on the pressure level) as shown by booms 1, 2 and 6. This however would need confirmation by dedicated studies. Second, an accurate control of boom reproduction in a real-life environment is all the more difficult as the boom level is lower, because a wider part of its spectrum mixes with the noise. This is again evidenced by booms 1, 2 and 6 with lower levels and larger deviations between target and measurement. The second main lesson of this comparison is that the present simulator with 7 loudspeakers is optimised for rooms of volumes around 30 m<sup>3</sup>, ideally bedrooms or small living rooms, with indoor transmission through wide open windows. It corresponds to a worst-case scenario (maximal indoor transmission) adapted to European houses (stiff walls and open windows). One could contemplate a “portable” version that could be affixed to private homes, so that short- and maybe medium-term low boom disturbances could be investigated while people living in their own homes. For ground-floor rooms, a simulator could be affixed outdoor in the house garden to one window. The obstruction of one window would make it best suited for investigating at-home sleep disturbances by sonic booms, an almost unexplored topic [16].

## 6 Conclusion

An electroacoustic system consisting in two simulators was designed to reproduce, with highest possible fidelity, low frequency, impulsive signals possibly with one or several sharp shocks. The objective was i) to cover a wide frequency range, here from 1 to 1500 Hz, ii) to reach sufficient peak amplitude (around 20 Pa), iii) to obtain good agreement for both the time signal and its spectrum, and iv) do this in different rooms of an existing home, for the purpose of

perception studies in a listening environment as realistic as possible. In addition to standard equalisation in the frequency domain, we used the WDT for optimisation in the time domain of the low frequency part of the signal. Target signals were those expected outdoor, thus assuming the signal is perceived indoor but with wide open windows. Two cases were investigated, with two different room volumes. For the smallest volume used to dimension the simulator, agreement between target and simulated signal is excellent. For the more demanding case of the largest volume, the agreement quality was reduced but the simulated signals were nevertheless clearly impulsive, with the desired time waveform with sharp shocks and the expected low frequency spectrum. The high frequency spectrum was however somewhat higher than the target one to reach the desired sound level (here A-SEL metric). The application was here the reproduction of sonic boom, but the proposed method can be applied to other low frequency and impulsive signals. The present study also raises the issue of influence of indoor background noise, existing in daily-life and usually ignored in laboratory studies, on boom reproduction, measurement and perception.

## Conflict of interest

The authors declare that they have no conflicts of interest in relation to this article.

## Data availability statement

Data are available on request from the authors.

## Acknowledgments

The RUMBLE project has received funding from the European Union’s Horizon 2020 research and innovation programme under Grant Agreement No. 769896. This document reflects only the authors’ view and the Commission is not responsible for any use that may be made of the information it contains. We would like to thank our colleagues in RUMBLE for the exchange during the preparation of this study, and in particular the project coordinator Jean-François Perelgritz (Airbus France),

Pierre-Elie Normand (Dassault-Aviation) for sharing the software computing various boom metrics, and Stephan Töpken (Carl von Ossietzky Universität Oldenburg) for his careful reading of the manuscript. Input signals 2, 3 and 5 were provided to us by Alexandra Loubeau (NASA Langley). Philippe Guibert, head of campus St Cyr of Sorbonne Université and Pierre-Yves Lagrée, director of Institut Jean Le Rond d’Alembert, are thanked for giving us access to the house for research purposes. Benjamin Véron (acoustical engineer at d’Alembert) is thanked for measuring reverberation times. The technical and administrative assistance of Jean-François Egéa, Jérôme Péquin, Jean-Marie Citerne, Hugo Dutilleul and Evelyne Mignon, all from Institut Jean Le Rond d’Alembert, were essential to carry out this study successfully. Anonymous reviewers are thanked for their relevant comments and suggestions that helped us improve this article.

## References

1. L.B. Jones: Lower bounds for sonic bangs. *Aeronautical Journal* 65, 606 (1961) 433–436.
2. A.R. George, R. Seebass: Sonic boom minimization including both front and rear shocks. *AIAA Journal* 9, 10 (1971) 2091–2093.
3. R. Seebass, A.R. George: Sonic boom minimization. *Journal of the Acoustical Society of America* 51 (1972) 686–694.
4. G.B. Whitham: The flow pattern of a supersonic projectile. *Communications on Pure and Applied Mathematics* 5, 3 (1952) 301–348.
5. J. Pawlowski, D. Graham, C. Boccadoro, P. Coen, D. Maglieri: Origins and overview of the shaped sonic boom demonstration program, in 43rd AIAA Aerospace Sciences Meeting and Exhibit, Paper AIAA-2005-0005, American Institute of Aeronautics and Astronautics, 2005, pp. 1–14.
6. M. Kanamori, T. Takahashi, Y. Naka, Y. Makino, H. Takahashi, H. Ishikawa: Numerical evaluation of effect of atmospheric turbulence on sonic boom observed in D-SEND# 2 flight test, in 55th AIAA Aerospace Sciences Meeting, Paper AIAA-2017-0278, American Institute of Aeronautics and Astronautics, 2017, pp. 1–10.
7. S.S. Stevens: Perceived level of noise by Mark VII and decibels (E). *Journal of the Acoustical Society of America* 51, 2C (1972) 575–601.
8. W. Doebler: Simulations of X-59 low-booms propagated through measured atmospheric profiles in Galveston, Texas. *Journal of the Acoustical Society of America* 148, 4 (2020) 2524–2524.
9. B.M. Sullivan: Research on subjective response to simulated sonic booms at NASA Langley Research Center. in: A.A. Atchley, V.W. Sparrow, R.M. Keolian (Eds.), *AIP Conference Proceedings*, vol. 838, American Institute of Physics, Melville, NY, 2006, pp. 659–6662.
10. D.J. Maglieri, P.J. Bobbitt, K.J. Plotkin, K.P. Shepherd, P.G. Coen, D.M. Richwine: Chapter 8: Response to sonic booms, in *Sonic boom: Six decades of research*, National Aeronautics and Space Administration, Hampton, VA, 2014, pp. 345–392.
11. J.D. Leatherwood, K.P. Shepherd, B.M. Sullivan: A new simulator for assessing subjective effects of sonic booms. Technical Report NASA TM-104150, 1991. Available at <https://ntrs.nasa.gov/api/citations/19920002541/downloads/19920002541.pdf>
12. Y. Naka: Subjective evaluation of loudness of sonic booms in-doors and outdoors. *Acoustical Science and Technology* 34, 3 (2013) 225–228.
13. S. Töpken, S. van de Par: Loudness and short-term annoyance of sonic boom signatures at low levels. *Journal of the Acoustical Society of America* 149, 3 (2021) 2004–2015.
14. J. Salamone: Portable sonic boom simulation. In: A.A. Atchley, V.W. Sparrow, R.M. Keolian Eds., *AIP Conference Proceedings*, Vol. 838, American Institute of Physics, Melville, NY, 2006, pp. 667–670.
15. B.M. Sullivan, P. Davies, K.K. Hodgdon, J.A. Salamone, A. Pilon: Realism assessment of sonic boom simulators. *Noise Control Engineering Journal* 56, 2 (2008) 141–157.
16. F. Coulouvrat: The challenges of defining an acceptable sonic boom overland, in 15th AIAA/CEAS Aeroacoustics Conference, Paper AIAA-2009-33842009, American Institute of Aeronautics and Astronautics, 2009, pp. 1–13.
17. A. Loubeau, J. Page: Human perception of sonic booms from supersonic aircraft. *Acoustics Today* 14 (2018) 23–30.
18. J.J. Gibson: *The ecological approach to visual perception*. Houghton Mifflin, Boston, 1979.
19. M.A. Schmuckler: What is ecological validity? A dimensional analysis. *Infancy* 2, 4 (2001) 419–436.
20. D.A. McCurdy, S.A. Brown, R.D. Hilliard: Subjective response of people to simulated sonic booms in their homes. *Journal of the Acoustical Society of America* 116, 3 (2004) 1573–1584.
21. J. Klos: Overview of an indoor sonic boom simulator at NASA Langley Research Center, INTER-NOISE and NOISE-CON Congress and Conference Proceedings 2012 (2012) 8973–8983.
22. V.W. Sparrow, S.L. Garrett: An audio reproduction grand challenge: design a system to sonic boom an entire house. In: 125th Audio Engineering Society Convention 2008, Paper 7607, Audio Engineering Society, 2008.
23. A. Loubeau, Y. Naka, B.G. Cook, V.W. Sparrow, J.M. Morgenstern: A new evaluation of noise metrics for sonic booms using existing data. *AIP Conference Proceedings* 1685 (2015) 090015.
24. M.A. Park, M. Nemeč: Nearfield summary and statistical analysis of the second AIAA sonic boom prediction workshop. *Journal of Aircraft* 56, 3 (2019) 851–875.
25. D. Luquet, R. Marchiano, F. Coulouvrat: Long range numerical simulation of acoustical shock waves in a 3D moving heterogeneous and absorbing medium. *Journal of Computational Physics* 379 (2019) 237–261.
26. R. Leconte, J.-C. Chassaing, F. Coulouvrat, R. Marchiano: Propagation of classical and low booms through kinematic turbulence with uncertain parameters, *Journal of the Acoustical Society of America* 151, 6 (2022) 4207–4227.
27. A. Tokuyama, K. Sakai, H. Taya: Experimental study of sonic boom acceptance. In: *Aircraft Design, Systems, and Operations Meeting*, Paper AIAA-93-3961, American Institute of Aeronautics and Astronautics, 1993.
28. C. Blanc, M.C. Remillieux, J.M. Corcoran, R.A. Burdisso: Generation of impulsive sound with speakers. *Noise Control Engineering Journal* 60, 2 (2012) 148–157.
29. K.A. Bradley, C.M. Hobbs, C.B. Wilmer, V.W. Sparrow, T.A. Stout, J.M. Morgenstern, K.H. Underwood, D.J. Maglieri, R. A. Cowart, M.T. Collmar, H. Shen, P. Blanc-Benon: Sonic booms in atmospheric turbulence (SonicBAT): The influence of turbulence on shaped sonic booms. NASA/CR-2020-220509, NASA Langley Research Center, Hampton, VA, NASA Langley Research Center, Hampton, VA, 2020.
30. S. Töpken, S. van de Par: Simulator for the reproduction of “low sonic boom”-signatures. In: *Forstschritte der Akustik – DAGA 2020*, Hannover, Germany, DEGA e.V., 2020, pp. 409–412.

## Appendix A

### Dimensions and reverberation times of the four rooms

**Table A1.** Dimensions of the four rooms.

Room	Length (m)	Width (m)	Height (m)
Bedroom 1	3.85	2.50	3.10
Bedroom 2	3.85	2.85	3.10
Living room	6.19	3.84	3.10
Kitchen	3.69	3.51	3.10

**Table A2.** Reverberation times  $T_{20}$  (s), measured according to ISO standard 3382-2 with an exploding balloon, per octave bands.

Octave band (Hz)	Bedroom 1	Bedroom 3	Living room	Kitchen
63	2.08	0.87	1.21	1.40
125	0.76	0.79	0.78	1.02
250	0.84	0.70	0.81	0.78
500	0.84	0.76	0.90	0.89
1000	0.75	0.68	0.87	0.93

## Appendix B

### Signal metrics

**Table B1.** Peak overpressure in Pa, and boom levels in dB (for ASEL, BSEL, CSEL, DSEL, ESEL, PL and ISBAP metrics) for the target (1st line/T) and measured (2nd line) boom signals investigated in this study. For each boom, W3 or F3 indicates the measurement points. Average level differences  $\Delta$  between measurement and target are indicated for each metric over the seven booms (last line) and for each boom over the seven dB metrics (last column).

Boom #	$p_{\max}$	ASEL	BSEL	CSEL	DSEL	ESEL	PL	ISBAP	$\Delta$
1 (T)	19.2	55.1	72.6	90.1	77.8	67.1	68.9	83.6	+2.8
1 (W3)	19.5	56.0	74.7	90.9	78.6	69.3	75.7	89.6	
2 (T)	19.4	61.7	76.2	91.2	79.0	71.6	76.2	88.6	+1.6
2 (W3)	19.8	61.9	77.8	92.4	80.1	72.9	78.9	91.8	
3 (T)	25.0	69.3	83.1	95.9	83.8	78.5	85.3	96.5	+0.1
3 (W3)	23.6	69.2	83.2	95.7	83.7	78.6	85.8	96.9	
4 (T)	23.8	74.3	85.5	94.1	85.2	82.5	86.7	95.0	+0.3
4 (W3)	24.3	74.5	85.4	94.6	85.2	82.1	87.4	96.2	
5 (T)	23.9	78.8	88.8	97.1	88.4	86.1	91.7	99.4	+0.4
5 (W3)	23.9	78.4	89.2	97.7	88.8	86.2	92.2	100.3	
6 (T)	17.3	62.2	79.7	93.1	80.8	74.2	77.7	90.7	+0.9
6 (F3)	12.3	63.2	79.7	92.0	80.1	74.5	81.5	93.4	
7 (T)	18.4	75.1	86.1	95.0	85.6	83.0	88.4	96.7	0
7 (F3)	14.9	75.0	85.6	94.6	85.2	82.6	89.2	97.5	
$\Delta$		+0.2	+0.5	+0.2	+0.1	+0.5	+2.3	+2.2	

**Cite this article as:** Cretagne L. García A.C. Leconte R. Ollivier F. Marchal J, et al. 2023. Design of a low frequency, impulsive sound simulator in an existing house for sonic boom perceptual studies. Acta Acustica, 7, 61.